Determination of the heat density of centralized heat networks in Austria 2050 under the 1.5°C climate target

Sebastian Zwickl-Bernhard[a,b,*], Daniel Huppmann[b], Antonia Golab[a], Hans Auer[a]

[a] *Energy Economics Group (EEG), Technische Universität Wien, Gusshausstrasse 25-29/E370-3, 1040 Wien, Austria*
[b] *Energy, Climate and Environment (ECE) Program, International Institute for Applied Systems Analysis (IIASA), Laxenburg, Austria*

Abstract

Achieving the 1.5 °C climate target requires, among others, a sustainable transformation of the heat supply. We downscale different European decarbonization scenarios of the heating sector to the Austrian grid level, using tailor-made downscaling techniques accounting for infrastructure requirements of renewable heat sources and the topology of centralized heat networks. We demonstrate that district heating networks are crucial in the highly efficient decarbonized heat supply in Austria in 2050 and identify eight different representative district heating networks, supplying heat demand between 0.6 and 12 TWh. Nevertheless, seven of these networks do not reach the heat density required for economic and technical efficiency from today's techno-economic perspective. We conclude that the decarbonization leads to centralized heat networks with lower heat densities.

Keywords: Centralized heat networks, heat density, district heating, 1.5°C climate target, downscaling, 2050

*Corresponding author
Email address: zwickl@eeg.tuwien.ac.at (Sebastian Zwickl-Bernhard)

Nomenclature

Type	Description	Unit
Set and index		
$t \in \mathcal{T} = \{1, \ldots, T\}$	Set of heat generation technologies/sources, index by t	
$r \in \mathcal{R} = \{1, \ldots, R\}$	Set of sub-regions, index by r	
$s \in \mathcal{S} = \{0, 1, *\}$	Stage of iterations, index by s	
Variables		
q_t	Heat generation per t	TWh
ρ_r	Population density per r	$1//\text{km}^2$
p_r	Total population per r	1
σ_t	Minimal network infrastructure requirements per t	$1//\text{km}^2$
π_r	Available potential of heat network infrastructure per r	$1//\text{km}^2$
$\hat{q}_{t,r}$	Heat generation per t and r	TWh
q_r^{heat}	Heat demand per r	TWh
$\tilde{q}_t$	Available heat generation per t	TWh
G^s	Centralized heat network graph at s	
n^s	Node of centralized heat network graph at s	
$l_{k,j}^s$	Line connecting nodes k and j at s	
$q_{n^s}^s$	Nodal centralized heat generation at s	TWh
$\tilde{q}_{n^s}^s$	Nodal on-site heat generation at s	TWh
$\pi_{n^s}^s$	Nodal benchmark indicator value at s	1
α_{n^s}	Number of triangles with direct neighboring nodes	1
β_{n^s}	Number of connection lines to the graph	1

1. Introduction

To implement the Paris Climate Agreement [1] and the SR1.5 [2], the European Commission has set deep decarbonization targets together with national governments. In particular, the "EU Green Deal" describes the concrete goals in Europe, namely, a climate-neutral and resource-conserving economy and society (see, e.g., [3]). The overarching goal is emissions neutrality 2050. The principles of a net-zero society are based on three key points: (i) reduction of the energy demand (see, e.g., Oshiro et al. [4] and Grubler et al. [5]), (ii) deployment and generation of renewable energy technologies (see, e.g., Bakhtavar et al. [6]), and (iii) an increase in efficiency regarding the provision of energy services and the associated optimal utilization of sustainable energy sources.

To achieve these long-term ambitions, the European Commission recently presented "Fit for 55", a concrete roadmap to 2030. This program commits to a 55 % reduction in CO_2 emissions in 2030 compared to to those in 1990 [7]. The concrete measures affect almost all sectors of the energy system and should lead to a significant efficiency improvement and a massive overall reduction in fossil fuels. It implies, among others, binding annual targets to reduce energy consumption and to extend the already established EU emissions trading system (EU ETS) to new sectors. In addition to transportation, the building sector will be part of the EU ETS in the future. In the building sector, using the annual anchored emissions reduction, this means a defined roadmap to complete decarbonization of the heating and cooling demand, as these are the two reasons for emissions in this sector. In this paper, we look at what deep decarbonization of building heating demand may look like in 2050 in Austria and the implications of the corresponding sustainable energy mix for centralized heating networks.

1.1. Implications of decarbonization on the heating sector

The scope of changes required by 2030/2050 in the heating sector becomes even clearer at the national level. In Europe, the average share of renewable energies in the heating and cooling sector in 2018 is only just above 20 % on

average, for all EU member states [8]. It is, in fact, higher in some countries, for example, in Austria, it is above 34 %. However, fossil fuels continue to dominate there as well. To be even more specific for the heating sector, of the nearly 4,000,000 residential dwellings in Austria, more than 900,000 are heated with natural gas, and more than 500,000 with oil [9]. If these heating systems are converted to renewable energy supply by 2050, this corresponds to a retrofitting of 50,000 units per year, or more than 130 per day - only in Austria. To achieve this goal, measures that go beyond the electrification of heat and lead to an expansion of district heating networks are necessary, although substantial heat saving measures are installed [10].

Centralized heating networks are particularly advantageous for supplying densely populated or urban areas because of high heat densities there [11]. In addition to heat density, the connection rate is a key factor determining the efficiency of district heating/cooling networks and thus their implementation. For example, currently in Austria, at a connection rate of 90 %, 10 GWh/km^2 is used as a benchmark for supplying an area with district heating[1]. The reference value of 10 GWh/km^2 is in line with findings regarding district heating networks also from the Scandinavian region (Denmark, Sweden, and Finland) [12]. These are rough estimates, but they do allow an initial assessment of the economic viability or feasibility of a district heating network. In a detailed consideration and evaluation of district heating networks, numerous factors play a decisive role. Nussbaumer and Thalmann [13] thoroughly elaborate on the network design and its impact on the profitability of centralized heat networks. In their study, Laasasenaho et al. [14] emphasize the optimal location of heat generation units/sources within centralized heat networks, enabling a cost-optimized heat supply. Gopalakrishnan and Kosanovic [15] focus on the optimal heat generation technology dispatch. When examining the economic viability of district heating networks, building renovation measures must also be taken into account

[1] `http://www.austrian-heatmap.gv.at/ergebnisse/`

(see, e.g., [16] and [17]). Hietaharju et al. [18] recently show in their analysis that a $2-3\%$ building renovation rate per year results in a $19-28\%$ decrease of the long-term district heating demand. This also reduces the heat density. However, studies show that a reduction in heat density is not necessarily a barrier to district heating networks [19]. Reidhav and Werner [20] show how energy taxes can improve the profitability of sparse district heating networks in Sweden. Following these considerations and in light of ambitious CO_2 reduction targets, it can also be assumed that the rising CO_2 price can have an effect similar to the energy tax. Of course, this is valid only in the case of deep decarbonization of the generation mix feeding into centralized heat networks. Di Lucia and Ericsson [21] show that biomass significantly contributed to the decarbonization of the district heating network and replaced fossil fuels in the feed-in generation mix in Sweden. In their multi-criteria study, Ghafghazi et al. [22] also identify wood pellets as the optimal system option for fueling district heating networks. Eventually, the increasing cooling demand and the co-design of centralized networks for heating and cooling can also increase the economic viability of these and counteract the reduction of heat density from an economic point of view [23].

1.2. Implications of large-scale numerical model results at the local level

In many cases when it comes to the question of optimal solutions, researchers use numerical models. In general, these models strike a balance between complexity and aggregation. Integrated assessment models (IAMs) are large numerical models covering complex interrelationships between climate, society, economics, policy, and technology [24]. Wilkerson et al. [25] and van Vuuren et al. [26] deal with IAMs and their role in understanding global energy decarbonization pathways. Schwanitz [27] evaluates IAMs of global climate change and discusses, among others, the appropriate level of regional (spatial) aggregation of countries in the modeling analysis. Generalizing this aspect reveals an aspect already known but essential in the context of large numerical models. It becomes necessary for modelers to set priorities regarding the level of detail, which inevitably

creates trade-offs in the analysis regarding the granularity of temporal, spatial, and other dimensions [28]. Gambhir et al. [29] also highlight this aspect of aggregation bias in their critical review of IAMs. They propose, among others, that IAMs should be increasingly be supplemented with other models and analytical approaches. Not least for this reason, (large) energy models also play a significant role in the analysis of energy systems in the context of climate change. Compared to IAMs, they more strongly emphasize the level of detail in terms of techno-economic characteristics. However, the lack of granularity remains, that these (global) energy models consider only a highly aggregated spatial resolution. To name just two selected approaches, Capros et al. [30] (PRIMES) and Löffler et al. [31] (GENeSYS-MOD) provide energy system models focusing on the European energy system with a spatial resolution at the country level. Further approaches are needed to disaggregate results obtained at the country level to finer scales, such as districts, neighborhoods, and other local levels. In this context, Backe et al. [32] provided a novel approach in the context of merging local activities/behavior in sustainable local communities into a large energy system model (bottom-up linkage). In their study, they integrated local flexibility options into the global energy system model EMPIRE, which provides, in principle, only country-level resolution. This and other work confirms the emerging trend of making top-down and bottom-up linkages between different spatial-temporal levels of resolution to drive decarbonization across all sectors.

1.3. Objective and contribution of this work

Against this background, the core objective of this work is downscaling European decarbonization scenarios of the heating sector to the community/distribution grid level serving end-users in 2050. In particular, downscaling considers the highly efficient and local use of sustainable heat sources in centralized heat networks (e.g., co-firing hydrogen in cogeneration plants and large-scale waste utilization, etc.). In addition, the topography of district heating networks is of particular importance and plays a crucial role in applied downscaling. This

allows estimates of realistic decarbonized district heating networks in 2050 to be obtained, which can be compared with existing networks. Thereby, the heat density of district heating networks serves as a comparative indicator and permits a rough estimation of the changes needed for centralized heating networks considering the 1.5°C climate target. An Austrian case study is conducted, downscaling the results of the heating sector in 2050 from the large numerical energy system model GENeSYS-MOD, from the country to the community/distribution grid levels.

The method applied consists of three different scenario-independent downscaling techniques. In the first technique, proportional downscaling using population as proxy is used as the reference (section 2.1). In the second, a sequential downscaling approach is presented, disaggregating from the country level to the subregion level. Thereby, the population density and infrastructure requirements of heat technologies serve as additional criteria in the downscaling (section 2.2). Finally, an iterative downscaling algorithm is presented. The algorithm is based on graph-theory benchmarking and projects centralized heat supply at the local (community) level (section 2.3). Section 3 presents and discusses the results of this work. Sections 3.1 and 3.2 show heat generation by source at different spatial levels. Sections 3.3 and 3.4 present centralized heat networks at a high spatial granularity. Section 3.5 synthesizes the results of centralized heat networks and compares heat densities of centralized heat networks in 2050 with today's values. Section 4 concludes this work and provides an outlook for future work.

2. Materials and methods

This section explains the methodology developed in this work. Section 2.1 describes proportional spatial downscaling using population as a proxy. This downscaling technique is a well-established approach for disaggregation and is often used in scientific and practical studies. Building on this, section 2.2 presents the sequential downscaling and section 2.3 presents the iterative downscaling algorithm in detail. Finally, section 2.4 concludes this section and explains the open-source tools used in this work.

2.1. Proportional spatial downscaling using population as a proxy

Proportional downscaling is a well-established technique and is commonly used. Equation 1 shows the primary expression of proportional downscaling, exemplarily, for the disaggregation of energy demand d from the country to the local levels, using population p as a proxy.

$$d_{local} = \frac{p_{local}}{p_{country}} \cdot d_{country} \tag{1}$$

The fields of application of proportional downscaling are not limited to the modeling of energy systems but to different fields of scientific and practical studies. The reason for this is the intuitive application and that it offers possibilities for tailor-made adaptions, in particular, related to the downscaling driver and proxy [33]. In this context, van Vuuren et al. [33] provide a comprehensive analysis of different proxies for the downscaling of global environmental change, including, among others, gross domestic product and emissions as a proxy. However, in the context of downscaling aggregated values of energy systems, one often finds proportional downscaling using population as a proxy (see, e.g., Ahn et al. [34], van Vuuren et al. [35], and Alam et al. [36]). For further information, we refer the reader to van Vuuren's study [35], providing a systematic classification of downscaling techniques going far beyond the simple proportional downscaling method discussed so far. The reader can find population-based downscaling in the authors' categorization under algorithmic and proportional downscaling. In

addition, they showed that novel downscaling methods have emerged in recent years as the scientific community has increasingly recognized the necessity for spatial and temporal disaggregation.

2.2. Sequential downscaling (from the country to the sub-region level)

The sequential downscaling algorithm (Algorithm 1) is developed to downscale the heat generation by source from the country to the sub-region levels. Before explaining the algorithm in detail, Table 1 provides an overview of the spatial nomenclature of this work using the European nomenclature of territorial units for statistics[2] (NUTS) and gives some examples of Austria. In particular, the different spatial levels of the applied downscaling are marked in gray. According to the NUTS nomenclature, Algorithm 1 downscales from the NUTS0 level to the NUTS3 level.

The purpose of the sequential downscaling algorithm is to provide a downscaling technique that considers the variation in efficiency of renewable heat sources and the increasing role of biomass and waste heat sources, in particular, in densely populated areas. Hence, we claim that

- limited amounts of hydrogen (and/or "green" gas) should preferably be used in district heating networks if they are used for heat supply (similar to Gerhardt et al. [37] and Zwickl-Bernhard and Auer [38]).
- high shares of biomass in the heating sector result in a high utilization rate of waste sources in waste incineration plants [39]. These waste incineration plants feed into district heating and therefore depend on the infrastructure of centralized heating networks (see, e.g., Sahlin et al. [40]).

Besides, we claim that high shares of air-source heat pumps (or geothermal sources) in the heat supply can only be realized if they are used as a co-firing heat source in district heating networks. We therefore consider two main aspects,

[2] `https://ec.europa.eu/eurostat/web/nuts/background`.

NUTS level	Description	Number	Example (population)
NUTS0	Country level	1	AT Austria (8.86 million)
NUTS1	Major socioeconomic regions	3	AT3 Western Austria (2.78 million)
NUTS2	Basic regions for the application of regional policies (federal states)	9	AT31 Upper Austria (1.48 million)
NUTS3	(Small) sub-regions for specific diagnoses (political/court districts)	35	AT312 Linz-Wels (529 thousand)
LAU (former NUTS4/5)	Subdivision of the NUTS 3 regions (communities)	2095	Enns AT312 Linz-Wels (11 thousand)

Table 1: Spatial nomenclature of different spatial levels using the NUTS nomenclature. Besides the number of regions per NUTS level, examples for the Austrian case study (incl. population) are given. The gray-colored rows mark the spatial levels used for downscaling in this work.

namely that geothermal sources will contribute significantly to decarbonizing the feed-in energy mix of existing district heating grids in the future (see, e.g., [41]), and that the provision of high shares of geothermal-based heat supply requires the distribution through district heating infrastructure [42]. Besides, it is highly uncertain whether small-scale geothermal units at the end-user's level will be economically viable in the future, because of the high investment costs expected.

To incorporate the abovementioned relevant technology-specific aspects, heat technologies/sources are downscaled according to their necessity of distribution infrastructure. Therefore, population density serves as a criterion, indicating the possibility of centralized heat networks. Table 2 provides a qualitative overview of the different heat generation technologies/sources and their heat network/infrastructure requirements.

Source / Heat technology	Requirements / Heat network	Rural / Sparsely	Town/Mixed / Moderate	Urban / Dense	Supporting references
Biomass	Middle		x	x	[43, 44, 39]
Direct electric	None	x	x	x	
Synthetic gas	Low	x	x	x	
Hydrogen	High			x	[45, 46, 47]
Heat pump (air)	None	x	x	x	[48]
Heat pump (ground)	High			x	[49, 50, 41]
Heat storage	None	x	x	x	

Table 2: Qualitative overview of heat generation technologies/sources and their requirements for heat network infrastructure. The prioritized preferences of heat sources in sub-regions are marked by the gray cell. In addition, selected references supporting this assumptions are cited.

The sub-regions used to downscale the corresponding heat sources are marked. Note that the different types are characterized by population density. Exemplarily, direct electric heating is a heat generation technology with no significant heat network requirements. It is downscaled to all types of sub-regions. In contrast, hydrogen is a heat source with high requirements and thus prioritized preferences (marked by the gray cell color). The right column refers to selected

references whose key findings are in line with this approach/these assumptions. Building on this, the sequential downscaling algorithm is presented below (Algorithm 1).

Algorithm 1: Sequential downscaling algorithm (NUTS0 to NUTS3)

t: Heat generation by technology/source ($t \in \mathcal{T}$);
r: Sub-region (or NUTS3 region) ($r \in \mathcal{R}$);

input : Heat generation by technology/source at NUTS0 level: (q_t);
Population density per sub-region r (ρ_r);
Total population per sub-region r (p_r);
Minimal network infrastructure requirements of t (σ_t);
Available potential of heat network infrastructure at r (π_r);

output: Heat generation by technology/source at NUTS3 level ($\hat{q}_{t,r}$);

Initialization:
Sort elements t in T descending by σ_t;
$q_r^{heat} \longleftarrow \sum_t q_t \cdot \frac{p_r}{\sum_r p_r}$; // Calculate heat demand at each sub-region
$\tilde{q}_t \longleftarrow q_t$; // Available heat generation for each technology/source
$\pi_r \longleftarrow \rho_r$; // Population density determines network potential

begin
  foreach t **do**
    $List = [\,]$; // Collect valid sub-regions
    $demand = 0$; // Remaining demand that needs to be covered
    $R^{'} = R \setminus \{\forall r \in R : \pi_r \leq \sigma_t\}$; // Get valid sub-regions by criteria
    foreach $r^{'} \in R^{'}$ **do**
      if $q_r^{heat} \geq 0$ **then**
        $List = List \cup r^{'}$; // Add valid sub-regions to collection
        $demand \mathrel{+}= q_r^{heat}$; // Total demand of valid sub-regions
      end
    end
    foreach $l \in List$ **do**
      $\hat{q}_{t,r} = \frac{q_r^{heat}}{demand} \cdot \tilde{q}_t$; // Population-based downscaling
      $q_r^{heat} \mathrel{-}= \hat{q}_{t,r}$; // Reduce heat demand at r
    end
  end
end

The inputs are as follows: (i) heat generation by technology/source at the NUTS0 level, (ii) population as well as population density at the NUTS3 level, and (iii) empirical assumptions in terms of network infrastructure requirements per heat technology/source and potentials for heat network infrastructure (see Table 2). The algorithm itself consists of three main parts: initialization, pre-calculations, and downscaling. First, the initialization of the algorithm sorts the heat generation technologies/sources in descending order in terms of network infrastructure requirements. Then, the calculation starts with the first technology/source (highest requirements) (line 6). For this technology/source, all possible sub-regions are collected (line 9). Those sub-regions already fully supplied (no remaining heat demand) are filtered out (line 11). After further pre-calculation steps, the available amount of heat generation is downscaled to all valid sub-regions using population as a proxy. This procedure is repeated sequentially for each heat technology/source. The outputs of the sequential downscaling algorithm are heat generation by source and the amount of heat demand covered by centralized heat networks at the NUTS3 level.

2.3. Iterative downscaling (from the sub-region to community levels)

This section explains the methodology of the iterative downscaling algorithm. We propose this downscaling technique projecting heat generation by technology/source from the sub-region (NUTS3) to the community levels (LAU) (see Table 1). This in-depth spatial resolution is imperative for realistic network infrastructure planning, as stated by Zvoleff et al. [51]. The underlying concept of iterative downscaling is based on graph theory and assessing network topology using benchmark indicators.

Algorithm 2: Iterative downscaling algorithm (NUTS3 to LAU level)

s: Stage of iteration ($s \in \{0, 1, *\}$);
G^s: Centralized heat network graph at stage s;
N^s: List of nodes at stage s: ($n^s \in N^s$);
L^s: List of lines connecting nodes k and j at stage s: ($l^s_{k,j} \in L^s$);
Q^s: Centralized heat generation at stage s: ($q^s_{n^s} \in Q^s$);
$\tilde{Q}^s$: On-site heat generation at stage s: ($\tilde{q}^s_{n^s} \in \tilde{Q}^s$);
Π^s: Benchmark indicator value at stage s ($\pi^s_{n^s} \in \Pi^s$);

input : $G^0 = \{N^0, L^0, Q^0, \tilde{Q^0}\}$;
output: $G^* = \{N^*, L^*, Q^*, \tilde{Q^*}\}$;

Initialization:
$s = 0$, $iter = True$;
begin
  while $iter = True$ **do**
    foreach $n \in N^s$ **do**
      $\Pi^s_{n^s} = f(N^s, L^s, Q^s)$; // Calculate benchmark indicator value
    end
    i with $\pi^s_i = min(\Pi^s)$; // Get node with lowest indicator value
    $N^{s+1} = N^s \setminus i$; // Remove node from graph obtaining next stage
    $\tilde{q} = \sum_{N^{s+1}} \tilde{q}^s_{n^s}$; // Calculate available on-site heat generation
    if $\tilde{q} \geq q^s_i$ **then**
      foreach n^{s+1} **do**
        $q^{s+1}_{n^{s+1}} = q^s_{n^s} + \frac{q^s_i}{\tilde{q}} \cdot \tilde{q}^s_{n^s}$; // Increase centralized heat amount
        $\tilde{q}^{s+1}_{n^{s+1}} = \tilde{q}^s_{n^s} - \frac{q^s_i}{\tilde{q}} \cdot \tilde{q}^s_{n^s}$; // Decrease on-site heat amount
      end
      $L^{s+1} = L^s \setminus \{\forall l^s_{k,j} : k = i \vee j = i\}$; // Remove connecting lines
      $G^{s+1} = \{N^{s+1}, L^{s+1}, Q^{s+1}, \tilde{Q^{s+1}}\}$; // Create new network graph
      $G^s = G^{s+1}$; // Set updated heat network graph as new input
    else
      $iterate = False$; // Stop iteration because of no reallocation
      $G^* = G^s$; // Set heat network graph as result
    end
  end
end

2.3.1. Algorithm description

The iterative downscaling algorithm is presented in Algorithm 2. The idea is to assess, benchmark, and improve the topology of centralized heat networks. This is achieved in our proposed approach by iterative downscaling. Essentially, the main steps of the algorithm can be summarized as follows:

1. Downscale the results of the sequential downscaling algorithm from the NUT3 to the LAU levels using population as the downscaling driver, to obtain the initial heat network graph G^0 (input).
2. Benchmark each node of the heat network graph (line 11), identify the node with the lowest indicator value, and remove the node from the graph, generating a reduced heat network graph (lines 13 and 14).
3. Check if the amounts of centralized and on-site heat generation can be reallocated (line 16).
4. If yes, reallocate centralized and on-site heat generation for all nodes (lines 18 and 19); otherwise stop algorithm.
5. Update heat network graph and jump to step 2.

Recent studies support this approach, focusing on the topography of energy systems and networks (see, e.g., [52]). Bordin et al. [53] conduct an approach for the optimized strategic network design of centralized heat systems. Allen et al. [55] evaluate the topology of centralized heating systems and conclude that the optimization of the topology is promising to facilitate the adoption of centralized heat networks.

2.3.2. Heat network topology benchmarking using a graph-theory-based indicator

So far, we have introduced only the function $f(N^s, L^s, Q^s)$ (see line 11 in the iterative algorithm (Algorithm 2)) as a calculation procedure of the benchmarking indicator value. Below, we describe and discuss the approach of using a weighted cluster coefficient as a function and benchmarking indicator.

The proposed benchmarking indicator value is derived from graph-theory. Detailed information in the context of network analysis using indicators can be found in the fundamental work by Strogatz in [56]. Morever, we refer the reader to Sanfeliu and Fu's study [57], in which network topologies and their transformation are described in detail. In this work, we use a weighted cluster coefficient as a benchmark indicator and determine the transformation path of the centralized heat network graph. Equation 2 shows the calculation of the

weighted cluster coefficient

$$c_{n^s} = \frac{q_{n^s}}{max\ q^s} \cdot \frac{\alpha_{n^s}}{\beta_{n^s}} \tag{2}$$

where q is the amount of centralized heat supply, α is the number of triangles that can be formed with direct neighboring nodes, and β is the number of lines connecting to the graph for node n at stage s. In the context of the fundamental concept of *alpha*, we refer again to the literature. In particular, the study in [58] comprehensively deals with cluster coefficients and provides related generalized concepts. In addition, relevant aspects of the cluster(ing) coefficient are shown in [59]. In the works cited and also in this study, the aim is to achieve a high value of the cluster coefficient for each node considered (i.e., $\frac{\alpha}{\beta} \approx 1$). However, we extend the basic concept of the cluster coefficient from the literature and propose a weighting with the relative centrally supplied heat quantity. From an energy economics point-of-view, at least two important aspects are considered in the benchmarking process: (i) a high connection rate to the centralized heat network and (ii) a connection of those areas to the network that have a high heat demand and heat density, respectively. Both aspects are investigated in the literature. For example, Nilsson et al. [60] focus on the importance of the connection rate of centralized heat networks. Besides, Dochev et al. [61] investigate the impact of linearly decreasing heat densities and the influence on the profitability of the centralized heat networks.

2.4. Development of an open-source package building on pyam

The method described will be released as an open-source Python package in the course of publishing this work at the author's GitHub account. In this package, we build on the existing open-source Python package *pyam* [62]. *Pyam* is an open-source package for the analysis and visualization of integrated assessment and macro-energy scenarios [63]. In this work, it is used particularly for (i) the linkage between the sequential and the iterative downscaling algorithms, (ii)

the internal calculation steps within both downscaling algorithms, and (iii) the visualization of the results. Besides, we used the open-source Python package *networkx* [64], when implementing the iterative downscaling algorithm. We refer to the repository for the codebase, data collection, and further information.

3. Results and discussion

This section presents the results of the Austrian case study. Four different storylines are investigated, covering a wide range of possible future developments of the Austrian energy system in the context of European deep decarbonization. Section 3.1 shows the heat generation mix supplying the heat demand (residential and commercial) at the country level. Section 3.2 describes the heat generation mix obtained on a more granular geographical scale, at sub-regional and community levels. Potentials of a centralized heat network are presented further in section 3.3. Section 3.4 shows the centralized heat networks at the community level. Finally, section 3.5 compares the projected centralized heat networks in 2050 with today's networks, based on heat density.

3.1. Heat supply of the Austrian residential and commercial sector in 2050: four different decarbonization scenarios obtained from the H2020 project openENTRANCE

This section presents the heat generation mix covering the Austrian residential and commercial heat demand in 2050 for four different storylines, which have been developed within the H2020 openENTRANCE project. They are named as follows: *Directed Transition*, *Societal Commitment*, *Techno-Friendly*, and *Gradual Development*. Within each of them, specific fundamental development of the energy systems is described while aiming for a sustainable transition of the provision of energy services. The first three storylines consider the achievement of the 1.5 °C global warming climate target. The last storyline (*Gradual Development*) can be interpreted as a more conservative storyline, aiming for the less ambitious 2.0 °C climate target. Below, the storylines are described

briefly, before the quantitative results at the country level are presented. For a more detailed description of the storylines, refer to [65] and [66]. Further information is also available on the website of the project [3] and GitHub[4].

The underlying concept of the four storylines is a three-dimensional space consisting of the following parameters: technology, policy, and society. Each storyline describes a specific pathway to reach a decarbonized energy system taking into account a pronounced contribution of two dimensions. Regarding the third dimension, a development is assumed that leads to no significant contribution to the decarbonization of the energy system.

- *Directed Transition* looks at a sustainable provision of energy services through strong policy incentives. This bundle of actions becomes necessary because neither the markets nor the society adequately pushes sustainable energy technologies.

- *Societal Commitment* achieves deep decarbonization of the energy system by a strong societal acceptance of the sustainable energy transition. Thereby, decentralized renewable energy technologies together with policy incentives lead to a sustainable supply of energy service needs. In parallel, no fundamental breakthroughs of new clean technologies are within sight.

- *Techno-Friendly* describes a development of the energy system where a significant market-driven breakthrough of renewable energy technologies gives rise to the decarbonization of energy service supply. Additionally, society acceptance supports the penetration of clean energy technologies and the sustainable transition.

- *Gradual Development* differs from the other storylines as on the one hand, this storyline aims only for the less ambitious 2.0 °C climate target, and on the other hand, a little of each possible sustainable development ini-

[3] `https://openentrance.eu/`
[4] `https://github.com/openENTRANCE`

tiative of the energy system is described here. Although the other three dimensions contribute to decarbonization, they do not push it sufficiently and result in a more conservative storyline than the others.

Table 3 shows the heat generation by technology/source in Austria in 2050 for the four different storylines. These values were obtained during the course of the H2020 project openENTRANCE and are the modeling results calculated using the open-source model GENeSYS-MODv2.0 [67]. According to the underlying assumptions in the storylines, the heat generation of the different sources/technologies varies significantly in some cases (e.g., hydrogen-based heat generation in *Directed Transition* and *Gradual Development* (7.62 TWh) or heat pump (ground) generation in *Techno-Friendly* and *Societal Commitment* (14.78 TWh)). The gray-colored column Σ presents the total heat generation using centralized heat networks, which varies between 19.49 TWh (*Techno-Friendly*) and 35.23 TWh (*Gradual Development*).

	Heat generation by source in TWh	Biomass	Direct Electric	Synthetic gas	Heat pump (air)	Heat pump (ground)	Heat storage	Hydrogen	Σ
Storyline	Directed Transition	5.37	2.13	0.36	22.73	19.50	14.84	1.03	25.90
	Societal Commitment	5.37	1.98	1.35	15.71	21.47	10.58	2.18	29.02
	Techno-Friendly	5.37	1.53	2.79	25.95	6.69	16.36	7.43	19.49
	Gradual Development	5.37	1.81	5.35	9.68	21.21	15.57	8.65	35.23

Table 3: Heat generation by source in TWh, supplying residential and commercial heat demands in Austria 2050 for the different scenarios. Values obtained from the H2020 project openENTRANCE and GENeSYS-MOD.

3.2. Heat technology generation in 2050 on different spatial granularities

Figure 1 shows the heat generation per technology/source on different spatial granularities: the country (NUTS0), sub-region (NUTS3), and community (LAU) levels (from left to right). The level of spatial details increases from the

left to the right. In the middle, the residential and commercial heat supply in representative rural and urban sub-regions, respectively, is presented. The rural sub-region *Mostviertel-Eisenwurzen* (NUTS3 code AT121) shows high shares of heat pumps (air sourced) and small-scale heat storage systems. In addition, synthetic gas and direct electric heating systems supply the heat demand. The urban sub-region *South Viennese environs* (AT127) is mainly supplied by ground-sourced heat pumps, biomass, and hydrogen. Air-sourced heat pumps and, again, heat storage cover the remaining demand. Throughout the pie charts within the figure, shares of heat generation using centralized heat networks are indicated using blue edges. On the extreme right, an example of the resulting centralized heat network at the community level for the four different scenarios is presented. Within the four subfigures presenting centralized heat networks (each for one storyline), the size of the points represents the amount of heat demand using centralized supply in a community. The comparably high heat demand in the *Gradual Development* scenario results in an extensive centralized heat network infrastructure (see lower right subfigure in Figure 1). The other three centralized heat networks are characterized by fewer (less supplied small sub-regions) and smaller points (less supplied heat demand by the centralized heat network). Figure 2 compares the heat generation by source between 2020 (today) and 2050 for the four different scenarios. The height of the bars shows the absolute differences by source between both years, whereby a negative difference indicates less heat generation by this source in 2050 for the *Societal Commitment* scenario. This scenario is more prominently presented as this scenario has the lowest total heat demand ($-18.15\,\mathrm{TWh}$). In addition, the scenarios with the lowest and highest differences, respectively, are marked for each heat source and the total demand. For instance, the highest decrease is seen in natural gas in the *Directed Transition* scenario ($-53.76\,\mathrm{TWh}$).

3.3. Sub-regions in Austria 2050 with high potentials for centralized heat supply

The potentials for centralized heat supply in Austria in 2050 are limited to densely populated areas (urban areas). In particular, the results indicate eight

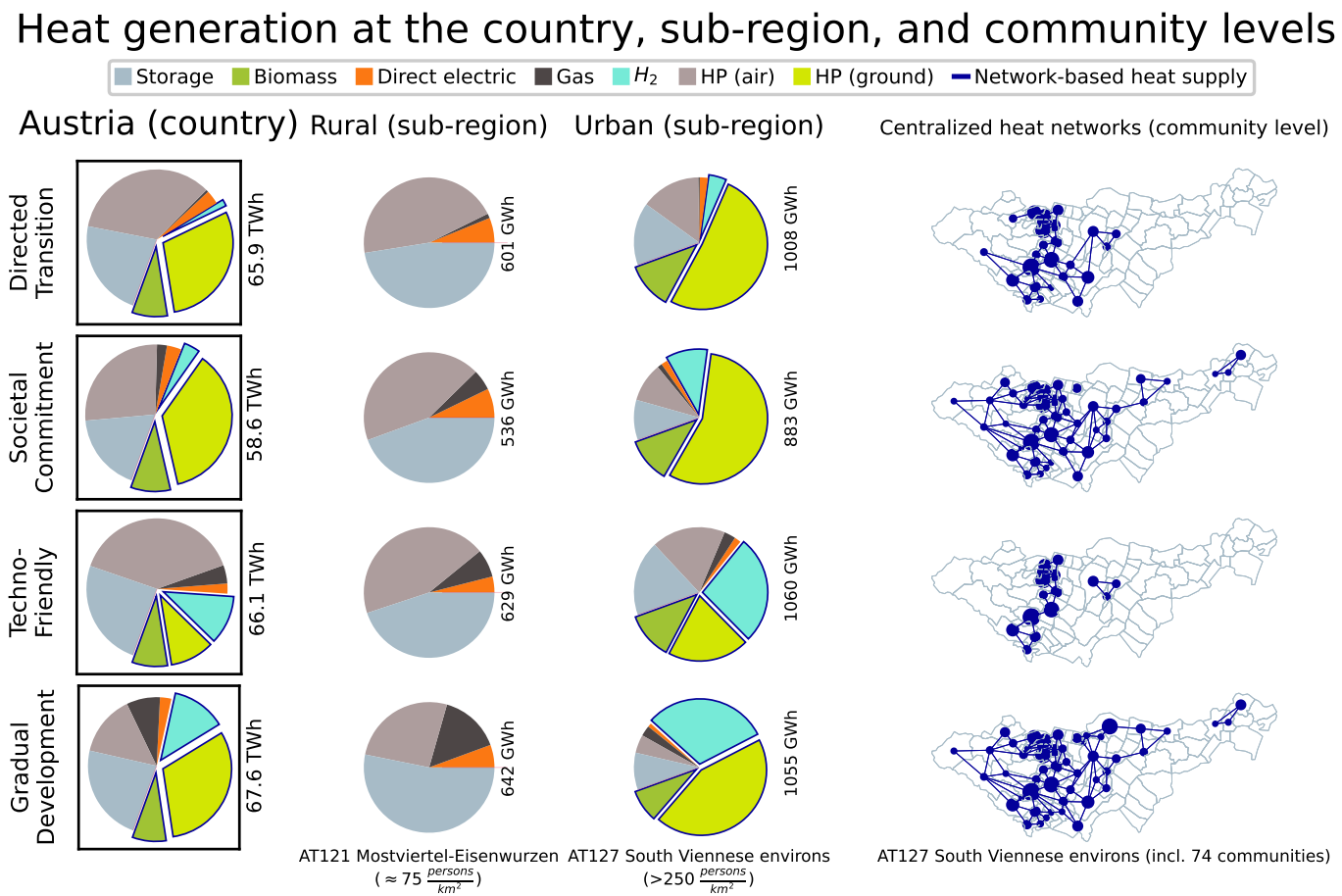

Figure 1: Heat technology generation on different spatial granularity levels in the different scenarios supplying the residential and commercial heat demand. left: on the country level. middle: comparison of a rural and urban sub-region. right: centralized heat network topology (size of the points represent the amount of heat demand supplied by the network)

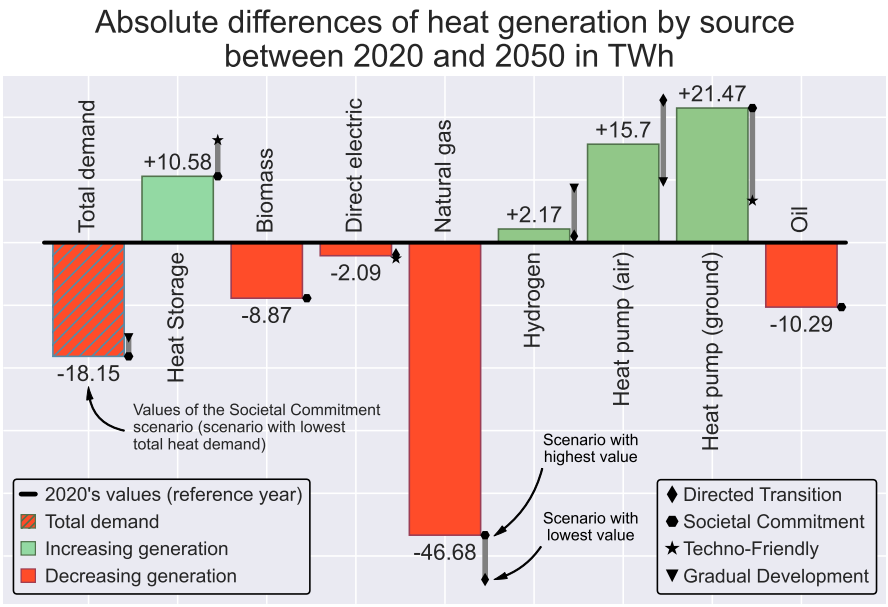

Figure 2: Comparison of heat generation by source between the reference year 2020 (black line) and 2050 in Austria. The height of the bars shows the absolute increase/decrease in 2050 in the *Societal Commitment* scenario. The scenarios with the lowest and highest differences, respectively, are indicated by the markers.

different sub-regions (NUTS3 regions) that are supplied by centralized heat networks (see Figure 3). Although the exact numerical numbers differ, the eight sub-regions in each scenario are (partially) supplied by centralized heat networks. Table 4 shows the centralized and on-site (decentralized) heat supply in the sub-regions. Thereby, the connection rate is assessed by the share of centralized heat supply in the total heat demand. Note that the population density varies in these sub-regions between 163 persons/km^2 (AT211 - Klagenfurt-Villach) and 5124 persons/km^2 (AT130 - Vienna).

3.4. Centralized heat network topology at the community level

This section presents the centralized heat network topology of the sub-region *South Viennese environs* (AT127) and all included communities. In Figure 3, this particular sub-region is marked by the orange box. Figure 4 shows the projected centralized heat network topology. In particular, the network topology is presented for the initial condition (as a result of the sequential downscaling, $i = 1$) and the final condition ($i = 51$) of the network. The distribution of the benchmark indicator values of the centralized heat network depending on the number of iterations is presented in the middle. The mean value is marked in orange. The supply area decreases with an increasing number of iterations. In the final condition, 25 communities are connected (starting from 75 in the initial condition). The number of connected population decreases by 38 %, starting from a population of 386.000 being connected to the centralized heating network in the initial condition. After the final iteration ($i = 51$), the termination criterion is reached. Note that the iterative reduction of small sub-regions supplied does not necessarily result in one contiguous graph (see the network graph in the *Gradual Development* scenario in Figure 1).

3.5. Comparison of 2050's and today's centralized heat networks using heat density as a criteria

In the following, the centralized heat network in *Graz* (AT221) is investigated in detail. This area is selected as it provides representative results in terms of both

Sub-region	Storyline	in TWh		in %
		Centralized	On-site	Connection rate
South Viennese environs (AT127)	Directed Transition	1.56	1.01	61
	Societal Commitment	1.80	0.49	79
	Techno-Friendly	1.13	1.45	44
	Gradual Development	2.28	0.36	86
Vienna (AT130)	Directed Transition	8.60	5.58	61
	Societal Commitment	9.90	2.70	79
	Techno-Friendly	6.25	7.80	44
	Gradual Development	12.57	1.96	87
Klagenfurt-Villach (AT211)	Directed Transition	1.31	0.90	60
	Societal Commitment	1.50	0.46	77
	Techno-Friendly	0.56	1.66	25
	Gradual Development	1.83	0.43	81
Graz (AT221)	Directed Transition	1.99	1.29	61
	Societal Commitment	2.30	0.62	79
	Techno-Friendly	1.45	1.85	44
	Gradual Development	2.92	0.46	86
Linz-Wels (AT312)	Directed Transition	2.68	1.74	61
	Societal Commitment	3.09	0.84	44
	Techno-Friendly	1.95	2.49	44
	Gradual Development	3.92	0.61	87
Salzburg and surroundings (AT323)	Directed Transition	1.61	1.05	61
	Societal Commitment	1.86	0.51	78
	Techno-Friendly	1.17	1.49	44
	Gradual Development	2.36	0.37	86
Innsbruck (AT332)	Directed Transition	1.36	0.93	59
	Societal Commitment	1.56	0.48	76
	Techno-Friendly	0.58	1.72	25
	Gradual Development	1.90	0.45	81
Rheintal-Bodensee (AT342)	Directed Transition	1.42	0.92	61
	Societal Commitment	1.64	0.45	78
	Techno-Friendly	1.03	1.32	44
	Gradual Development	2.08	0.32	87

Table 4: Centralized heat supply and on-site heat generation in the eight Austrian sub-regions, with potentials of centralized heat networks in 2050

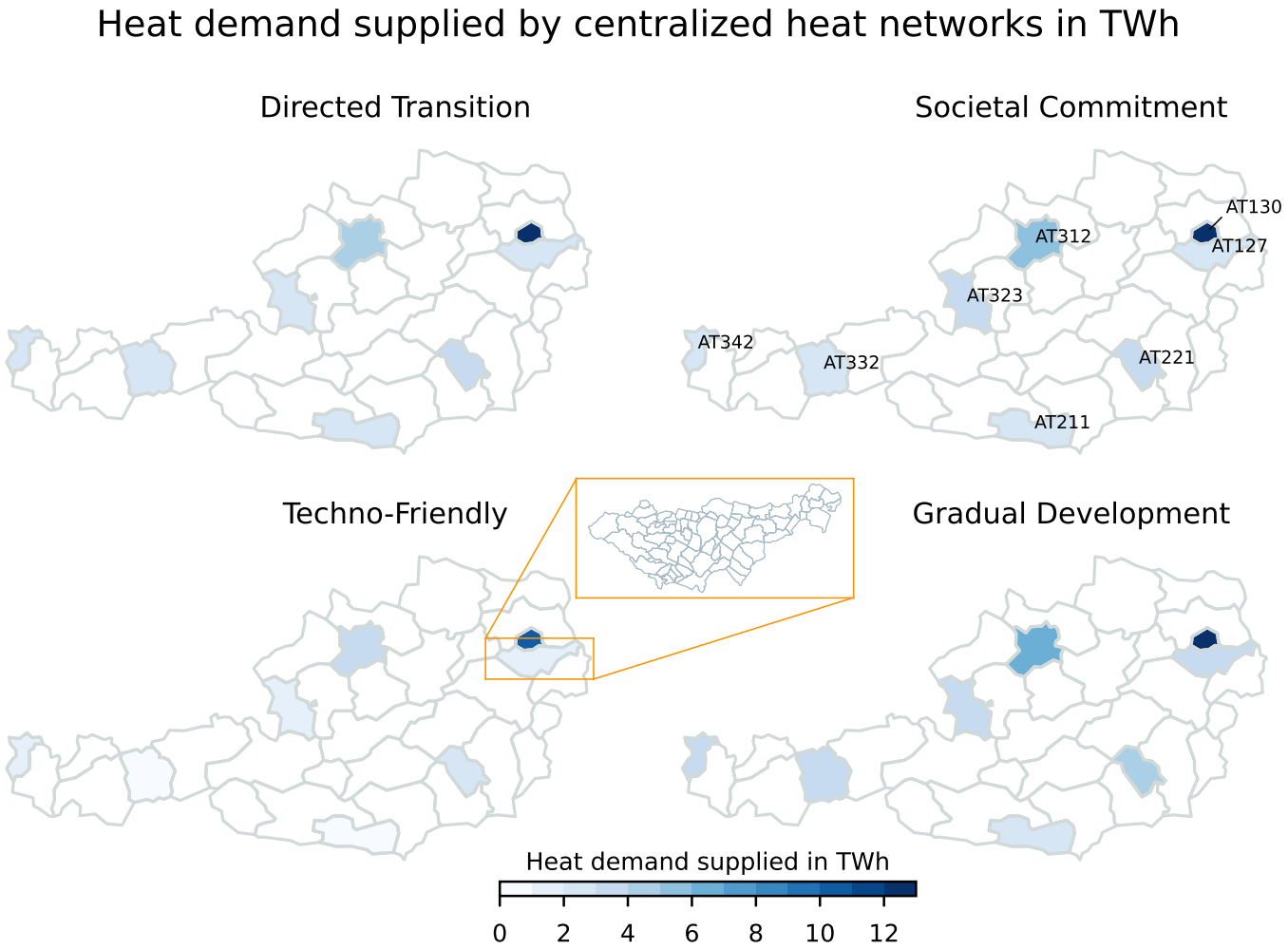

Figure 3: Heat demand supplied by centralized heat networks in Austria 2050. The white areas are supplied by on-site (decentralized) sustainable heat generation technologies/sources.

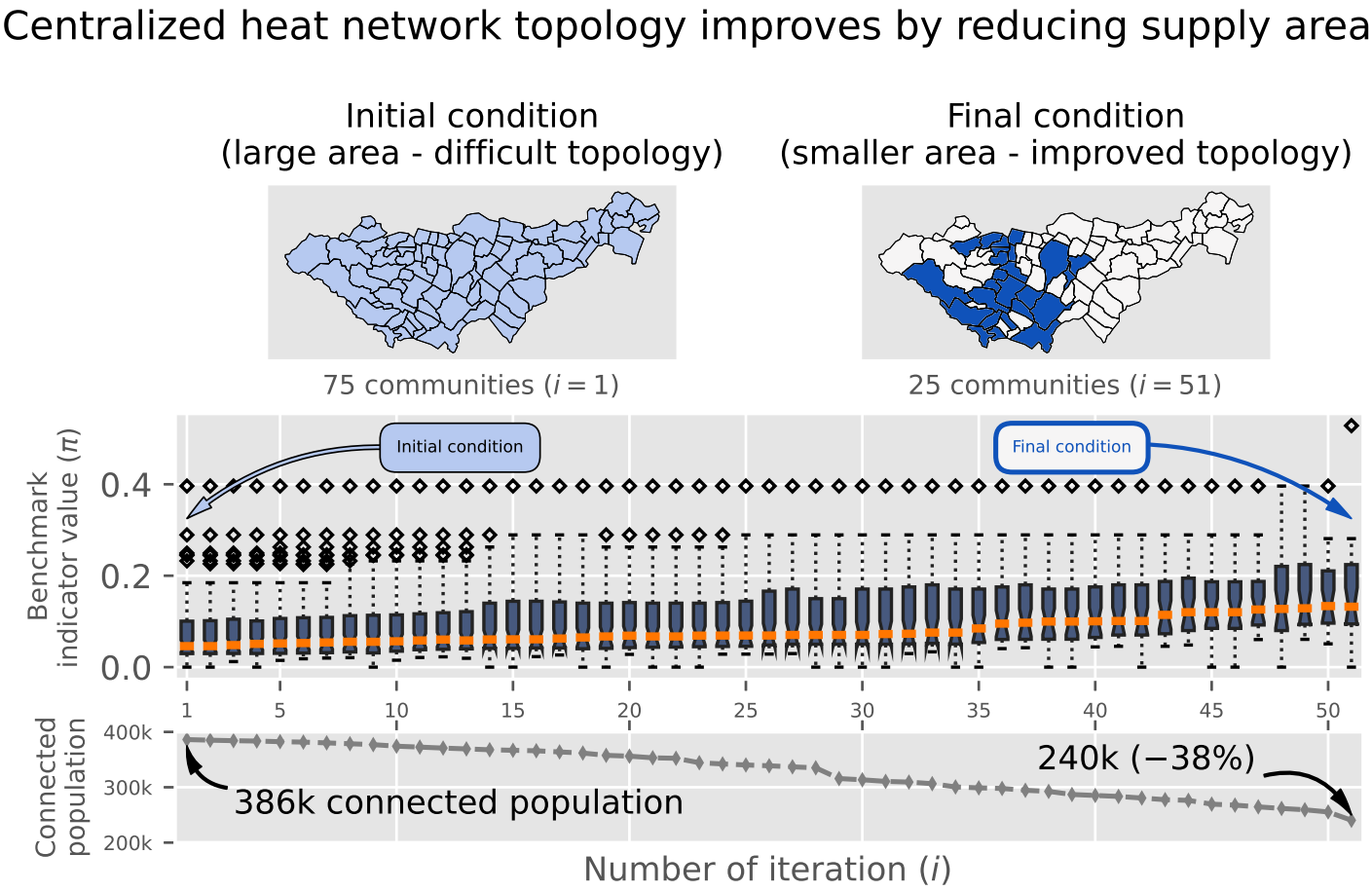

Figure 4: Centralized heat network topology in the initial and final condition. The boxplot (middle) indicates the improved network topology by an increasing benchmark indicator mean value (orange line). In the final condition, the connected population declines by −13.3 % compared to the initial condition.

the applied downscaling and achievable heat density benchmarks of centralized heat networks. Figure 5 shows the heat density of the centralized heat network in the *Techno-Friendly* scenario.

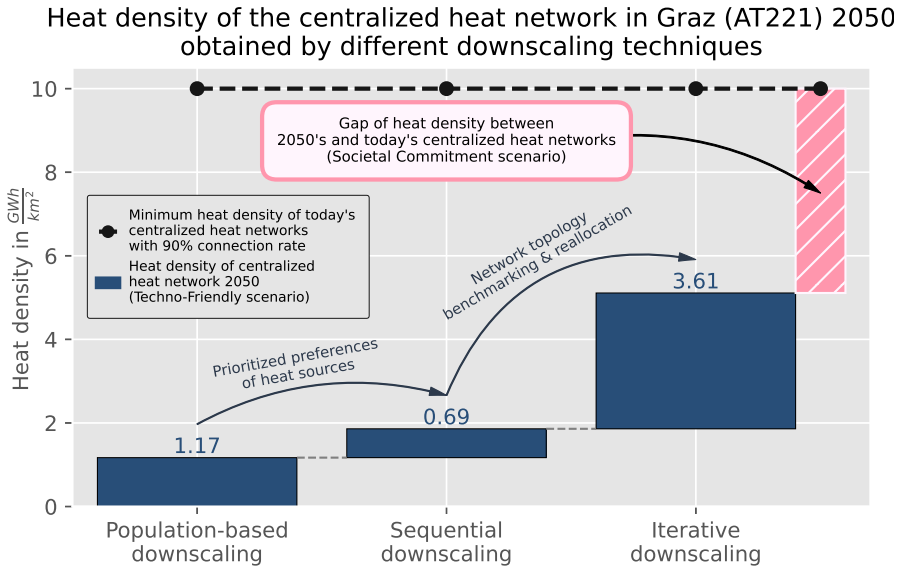

Figure 5: Heat density of the centralized heat network in *Graz* (AT221) 2050 in the *Techno-Friendly* scenario. The gap of heat density between 2050s and today (black dashed line) is marked by the pink bar.

The x-axis shows the three different downscaling techniques. The numerical numbers indicate a significant increase of the heat density by the sequential ($+0.69\,\mathrm{GWh/km^2}$) and, in particular, the iterative downscaling ($+3.61\,\mathrm{GWh/km^2}$). However, comparing the heat density value obtained with the heat density values of today's centralized heat networks reveals a significant gap (see the hatched pink bar). Here, in the *Techno-Friendly* scenario, it is $4.53\,\mathrm{GWh/km^2}$. According to references from the practice (see, e.g., in `http://www.austrian-heatmap.gv.at/ergebnisse/`), the heat density of today's networks is assumed to be $10\,\frac{\mathrm{GWh}}{\mathrm{km^2}}$ with a connection rate of 90 %. The gap of heat density varies between the different scenarios. Figure 6 shows the heat densities in the sub-regions and compares the results in the different scenarios. It shows the scenarios with

the lowest and highest heat densities. The bottom bar shows the value and scenario with the lowest heat density among the four different scenarios for each sub-region. The hatched bar indicates the increase of heat density and the corresponding scenario compared to the lowest value. In five sub-regions, the *Techno-Friendly* scenario is the scenario with the lowest heat density. The *Directed Transition* scenario is the scenario with the highest heat density in four sub-regions. Note that Vienna (AT130) is not shown for the sake of clarity. The heat density there varies between 15.1 $\frac{\text{GWh}}{\text{km}^2}$ in the *Techno-Friendly* and 30.3 $\frac{\text{GWh}}{\text{km}^2}$ in the *Gradual Development* scenario.

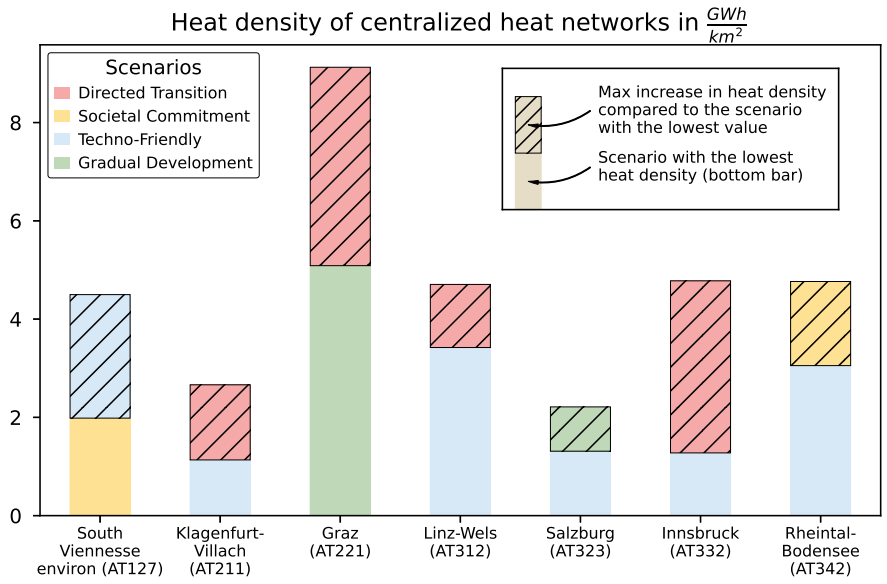

Figure 6: Comparison of the heat density in different scenarios for each sub-region. The bottom bar shows the scenario with the lowest heat density. The hatched bar indicates the increase of heat density and the corresponding scenario compared to the lowest value.

4. Conclusions and recommendations

Sustainable energy transition requires methods to bridge the gap between global decarbonization plans and the resulting necessary measures at the local level. This work emphasizes the development of different downscaling algorithms in

general, and the downscaling of the Austrian heating sector (residential and commercial) under the 1.5°C climate target to the community and grid levels in particular, considering technology-specific infrastructure requirements for the highly efficient usage of heat sources.

We found that the prioritized perspective of efficiency and local utilization of renewable heat sources leads to a crucial treatment of the further development of district heating networks in the decarbonized Austrian heat supply toward 2050. This implies small-scale ($< 1\,\mathrm{TWh}$) and large-scale ($> 12\,\mathrm{TWh}$) district heating networks in terms of the amount of heat delivered. The results demonstrate that particularly densely populated areas are still beneficial supply areas for district heating networks and offer adequate heat densities. Nevertheless, most district heating networks in 2050 (seven of eight) will not reach the heat density benchmarks of today's networks and have a significant heat density gap. However, considering the increasing importance of local renewable heat sources feeding into district heating networks, we assume that these centralized networks will become required in the future and crucial in the decarbonization of the heating sector.

We anticipate our work as a starting point, discussing the role of centralized heat networks as an infrastructure hub in the light of enabling large-scale, highly efficient, and local integration of renewable heat sources (such as biomass/waste, hydrogen, ground-sourced heat pumps, or geothermal units). In particular, we see a need for further research on the trade-off analysis between the efficiency/local integration of heat sources and the cost-intensive deployment of district heating networks. Future work may elaborate on the increasing cooling demand and how the cooperative design of district heating and cooling networks can contribute to the profitability of centralized heating and cooling infrastructure.

Declaration of interests

None.

Declaration of Competing Interest

The authors report no declarations of interest.

Acknowledgments

This project has received funding from the European Union's Horizon 2020 Research and Innovation Programme under Grant Agreement No. 835896. Part of the research was developed in the Young Scientists Summer Program (YSSP) at the International Institute for Applied Systems Analysis(IIASA), Laxenburg (Austria). The authors acknowledge TU Wien Bibliothek for financial support through its Open Access Funding Programme.

References

[1] Agreement, Paris, Paris agreement, in: Report of the Conference of the Parties to the United Nations Framework Convention on Climate Change (21st Session, 2015: Paris). Retrived December, Vol. 4, HeinOnline, 2015, p. 2017.

[2] O. Edenhofer, R. Pichs-Madruga, Y. Sokona, K. Seyboth, P. Matschoss, S. Kadner, T. Zwickel, P. Eickemeier, G. Hansen, S. Schlömer, et al., IPCC special report on renewable energy sources and climate change mitigation, Prepared By Working Group III of the Intergovernmental Panel on Climate Change, Cambridge University Press, Cambridge, UK (2011).

[3] C. Kemfert, Green deal for europe: More climate protection and fewer fossil fuel wars, Intereconomics 54 (6) (2019) 353–358. doi:https://doi.org/10.1007/s10272-019-0853-9.

[4] K. Oshiro, S. Fujimori, Y. Ochi, T. Ehara, Enabling energy system transition toward decarbonization in japan through energy service demand reduction, Energy 227 (2021) 120464. doi:https://doi.org/10.1016/j.energy.2021.120464.

[5] A. Grubler, C. Wilson, N. Bento, B. Boza-Kiss, V. Krey, D. L. McCollum, N. D. Rao, K. Riahi, J. Rogelj, S. De Stercke, et al., A low energy demand scenario for meeting the 1.5 c target and sustainable development goals without negative emission technologies, Nature energy 3 (6) (2018) 515–527. doi:https://doi.org/10.1038/s41560-018-0172-6.

[6] E. Bakhtavar, T. Prabatha, H. Karunathilake, R. Sadiq, K. Hewage, Assessment of renewable energy-based strategies for net-zero energy communities: A planning model using multi-objective goal programming, Journal of Cleaner Production 272 (2020) 122886. doi:https://doi.org/10.1016/j.jclepro.2020.122886.

[7] European Commission, COMMUNICATION FROM THE COMMISSION TO THE EUROPEAN PARLIAMENT, THE COUNCIL, THE EUROPEAN ECONOMIC AND SOCIAL COMMITTEE AND THE COMMITTEE OF THE REGIONS 'Fit for 55': delivering the EU's 2030 Climate Target on the way to climate neutrality, retrieved on 04.09.2021, https://eur-lex.europa.eu/legal-content/EN/TXT/?uri=CELEX:52021DC0550 (2021).

[8] Eurostat, Share of energy from renewable sources, retrieved on 08.09.2021, https://ec.europa.eu/eurostat/web/products-eurostat-news/-/ddn-20200211-1 (2021).

[9] Statistik Austria, Heizungen 2003 bis 2020 nach Bundesländern, verwendetem Energieträger und Art der Heizung, retrieved on 08.09.2021, https://www.statistik.at/wcm/idc/idcplg?IdcService=GET_PDF_FILE&RevisionSelectionMethod=LatestReleased&dDocName=022721 (2020).

[10] F. Jalil-Vega, A. D. Hawkes, Spatially resolved model for studying decarbonisation pathways for heat supply and infrastructure trade-offs, Applied Energy 210 (2018) 1051–1072. doi:https://doi.org/10.1016/j.apenergy.2017.05.091.

[11] S. Inage, Y. Uchino, Development of an integrated infrastructure simulator for sustainable urban energy optimization and its application, Sustainable Energy Technologies and Assessments 39 (2020) 100710. doi:https://doi.org/10.1016/j.seta.2020.100710.

[12] H. Zinko, B. Bøhm, H. Kristjansson, U. Ottosson, M. Rama, K. Sipila, District heating distribution in areas with low heat demand density, The 11th International Symposium on District Heating and Cooling, Reykjavik, Iceland (2008).

[13] T. Nussbaumer, S. Thalmann, Influence of system design on heat distribution costs in district heating, Energy 101 (2016) 496–505. doi:https://doi.org/10.1016/j.energy.2016.02.062.

[14] K. Laasasenaho, A. Lensu, R. Lauhanen, J. Rintala, Gis-data related route optimization, hierarchical clustering, location optimization, and kernel density methods are useful for promoting distributed bioenergy plant planning in rural areas, Sustainable Energy Technologies and Assessments 32 (2019) 47–57. doi:https://doi.org/10.1016/j.seta.2019.01.006.

[15] H. Gopalakrishnan, D. Kosanovic, Economic optimization of combined cycle district heating systems, Sustainable Energy Technologies and Assessments 7 (2014) 91–100. doi:https://doi.org/10.1016/j.seta.2014.03.006.

[16] I. Andrić, J. Fournier, B. Lacarrière, O. Le Corre, P. Ferrão, The impact of global warming and building renovation measures on district heating system techno-economic parameters, Energy 150 (2018) 926–937. doi:https://doi.org/10.1016/j.energy.2018.03.027.

[17] M. Rabani, H. B. Madessa, N. Nord, Achieving zero-energy building performance with thermal and visual comfort enhancement through optimization of fenestration, envelope, shading device, and energy supply system, Sustainable Energy Technologies and Assessments 44 (2021) 101020. doi:https://doi.org/10.1016/j.seta.2021.101020.

[18] P. Hietaharju, J. Pulkkinen, M. Ruusunen, J.-N. Louis, A stochastic dynamic building stock model for determining long-term district heating demand under future climate change, Applied Energy 295 (2021) 116962. doi:https://doi.org/10.1016/j.apenergy.2021.116962.

[19] U. Persson, S. Werner, Heat distribution and the future competitiveness of district heating, Applied Energy 88 (3) (2011) 568–576. doi:https://doi.org/10.1016/j.apenergy.2010.09.020.

[20] C. Reidhav, S. Werner, Profitability of sparse district heating, Applied Energy 85 (9) (2008) 867–877. doi:https://doi.org/10.1016/j.apenergy.2008.01.006.

[21] L. Di Lucia, K. Ericsson, Low-carbon district heating in sweden–examining a successful energy transition, Energy Research & Social Science 4 (2014) 10–20. doi:https://doi.org/10.1016/j.erss.2014.08.005.

[22] S. Ghafghazi, T. Sowlati, S. Sokhansanj, S. Melin, A multicriteria approach to evaluate district heating system options, Applied Energy 87 (4) (2010) 1134–1140. doi:https://doi.org/10.1016/j.apenergy.2009.06.021.

[23] D. Zhang, B. Zhang, Y. Zheng, R. Zhang, P. Liu, Z. An, Economic assessment and regional adaptability analysis of cchp system coupled with biomass-gas based on year-round performance, Sustainable Energy Technologies and Assessments 45 (2021) 101141. doi:https://doi.org/10.1016/j.seta.2021.101141.

[24] H. Dowlatabadi, Integrated assessment models of climate change: An in-

complete overview, Energy Policy 23 (4-5) (1995) 289–296. doi:https://doi.org/10.1016/0301-4215(95)90155-Z.

[25] J. T. Wilkerson, B. D. Leibowicz, D. D. Turner, J. P. Weyant, Comparison of integrated assessment models: carbon price impacts on US energy, Energy Policy 76 (2015) 18–31. doi:https://doi.org/10.1016/j.enpol.2014.10.011.

[26] D. P. Van Vuuren, H. Van Soest, K. Riahi, L. Clarke, V. Krey, E. Kriegler, J. Rogelj, M. Schaeffer, M. Tavoni, Carbon budgets and energy transition pathways, Environmental Research Letters 11 (7) (2016) 075002. doi:https://doi.org/10.1088/1748-9326/11/7/075002.

[27] V. J. Schwanitz, Evaluating integrated assessment models of global climate change, Environmental Modelling & Software 50 (2013) 120–131. doi:https://doi.org/10.1016/j.envsoft.2013.09.005.

[28] M. Gargiulo, B. Ó. Gallachóir, Long-term energy models: Principles, characteristics, focus, and limitations, Wiley Interdisciplinary Reviews: Energy and Environment 2 (2) (2013) 158–177. doi:https://doi.org/10.1002/wene.62.

[29] A. Gambhir, I. Butnar, P.-H. Li, P. Smith, N. Strachan, A review of criticisms of integrated assessment models and proposed approaches to address these, through the lens of BECCS, Energies 12 (9) (2019) 1747. doi:https://doi.org/10.3390/en12091747.

[30] P. Capros, N. Tasios, A. De Vita, L. Mantzos, L. Paroussos, Model-based analysis of decarbonising the EU economy in the time horizon to 2050, Energy Strategy Reviews 1 (2) (2012) 76–84. doi:https://doi.org/10.1016/j.esr.2012.06.003.

[31] K. Löffler, K. Hainsch, T. Burandt, P.-Y. Oei, C. Kemfert, C. Von Hirschhausen, Designing a model for the global energy

system—GENeSYS-MOD: an application of the open-source energy modeling system (OSeMOSYS), Energies 10 (10) (2017) 1468. doi:https://doi.org/10.3390/en10101468.

[32] S. Backe, M. Korpås, A. Tomasgard, Heat and electric vehicle flexibility in the European power system: A case study of Norwegian energy communities, International Journal of Electrical Power & Energy Systems 125 (2021) 106479. doi:https://doi.org/10.1016/j.ijepes.2020.106479.

[33] D. Van Vuuren, P. Lucas, H. Hilderink, D. P. van Vuuren, Downscaling drivers of global environmental change, Enabling use of global SRES scenarios at the national and grid levels. MNP Report 550025001 (2006) 2006.

[34] Y.-H. Ahn, J.-H. Woo, F. Wagner, S. J. Yoo, Downscaled energy demand projection at the local level using the iterative proportional fitting procedure, Applied Energy 238 (2019) 384–400. doi:https://doi.org/10.1016/j.apenergy.2019.01.051.

[35] D. P. van Vuuren, S. J. Smith, K. Riahi, Downscaling socioeconomic and emissions scenarios for global environmental change research: a review, Wiley Interdisciplinary Reviews: Climate Change 1 (3) (2010) 393–404. doi:https://doi.org/10.1002/wcc.50.

[36] M. S. Alam, P. Duffy, B. Hyde, A. McNabola, Downscaling national road transport emission to street level: A case study in dublin, ireland, Journal of Cleaner Production 183 (2018) 797–809. doi:https://doi.org/10.1016/j.jclepro.2018.02.206.

[37] N. Gerhardt, J. Bard, R. Schmitz, M. Beil, M. Pfennig, T. Kneiske, Hydrogen in the energy system of the future: Focus on heat in buildings, retrieved from Fraunhofer Institute for Energy Economics and Energy System Technology on 06.09.2021, https://www.iee.fraunhofer.de/en/presse-infothek/press-media/overview/2020/Hydrogen-and-Heat-in-Buildings.html (2020).

[38] S. Zwickl-Bernhard, H. Auer, Demystifying natural gas distribution grid decommissioning: An open-source approach to local deep decarbonization of urban neighborhoods, Energy (2021) 121805doi:https://doi.org/10.1016/j.energy.2021.121805.

[39] T. Fruergaard, T. H. Christensen, T. Astrup, Energy recovery from waste incineration: Assessing the importance of district heating networks, Waste Management 30 (7) (2010) 1264–1272. doi:https://doi.org/10.1016/j.wasman.2010.03.026.

[40] J. Sahlin, D. Knutsson, T. Ekvall, Effects of planned expansion of waste incineration in the swedish district heating systems, Resources, Conservation and Recycling 41 (4) (2004) 279–292. doi:https://doi.org/10.1016/j.resconrec.2003.11.002.

[41] J. M. Weinand, M. Kleinebrahm, R. McKenna, K. Mainzer, W. Fichtner, Developing a combinatorial optimisation approach to design district heating networks based on deep geothermal energy, Applied Energy 251 (2019) 113367. doi:https://doi.org/10.1016/j.apenergy.2019.113367.

[42] F. Dalla Longa, L. P. Nogueira, J. Limberger, J.-D. van Wees, B. van der Zwaan, Scenarios for geothermal energy deployment in europe, Energy 206 (2020) 118060. doi:https://doi.org/10.1016/j.energy.2020.118060.

[43] I. Vallios, T. Tsoutsos, G. Papadakis, Design of biomass district heating systems, Biomass and bioenergy 33 (4) (2009) 659–678. doi:https://doi.org/10.1016/j.biombioe.2008.10.009.

[44] K. Ericsson, S. Werner, The introduction and expansion of biomass use in swedish district heating systems, Biomass and bioenergy 94 (2016) 57–65. doi:https://doi.org/10.1016/j.biombioe.2016.08.011.

[45] I. G. Jensen, F. Wiese, R. Bramstoft, M. Münster, Potential role of renewable gas in the transition of electricity and district heating systems,

Energy Strategy Reviews 27 (2020) 100446. doi:https://doi.org/10.1016/j.esr.2019.100446.

[46] P. E. Dodds, I. Staffell, A. D. Hawkes, F. Li, P. Grünewald, W. McDowall, P. Ekins, Hydrogen and fuel cell technologies for heating: A review, International Journal of Hydrogen Energy 40 (5) (2015) 2065–2083. doi:https://doi.org/10.1016/j.ijhydene.2014.11.059.

[47] A. Arsalis, Thermodynamic modeling and parametric study of a small-scale natural gas/hydrogen-fueled gas turbine system for decentralized applications, Sustainable Energy Technologies and Assessments 36 (2019) 100560. doi:https://doi.org/10.1016/j.seta.2019.100560.

[48] Y. Yang, J. Ren, H. S. Solgaard, D. Xu, T. T. Nguyen, Using multicriteria analysis to prioritize renewable energy home heating technologies, Sustainable Energy Technologies and Assessments 29 (2018) 36–43. doi:https://doi.org/10.1016/j.seta.2018.06.005.

[49] S. A. Kyriakis, P. L. Younger, Towards the increased utilisation of geothermal energy in a district heating network through the use of a heat storage, Applied Thermal Engineering 94 (2016) 99–110. doi:https://doi.org/10.1016/j.applthermaleng.2015.10.094.

[50] J. Unternährer, S. Moret, S. Joost, F. Maréchal, Spatial clustering for district heating integration in urban energy systems: Application to geothermal energy, Applied Energy 190 (2017) 749–763. doi:https://doi.org/10.1016/j.apenergy.2016.12.136.

[51] A. Zvoleff, A. S. Kocaman, W. T. Huh, V. Modi, The impact of geography on energy infrastructure costs, Energy Policy 37 (10) (2009) 4066–4078. doi:https://doi.org/10.1016/j.enpol.2009.05.006.

[52] M. Abuelnasr, W. El-Khattam, I. Helal, Examining the influence of microgrids topologies on optimal energy management systems decisions using

genetic algorithm, Ain Shams Engineering Journal 9 (4) (2018) 2807–2814. doi:https://doi.org/10.1016/j.asej.2017.09.002.

[53] C. Bordin, A. Gordini, D. Vigo, An optimization approach for district heating strategic network design, European Journal of Operational Research 252 (1) (2016) 296–307. doi:https://doi.org/10.1016/j.ejor.2015.12.049.

[54] O. Shekoofa, S. Karbasian, Design criteria for electrical power subsystem's topology selection, in: 2013 6th International Conference on Recent Advances in Space Technologies (RAST), IEEE, 2013, pp. 559–564. doi:https://doi.org/10.1109/RAST.2013.6581274.

[55] A. Allen, G. Henze, K. Baker, G. Pavlak, Evaluation of low-exergy heating and cooling systems and topology optimization for deep energy savings at the urban district level, Energy Conversion and Management 222 (2020) 113106. doi:https://doi.org/10.1016/j.enconman.2020.113106.

[56] S. H. Strogatz, Exploring complex networks, Nature 410 (6825) (2001) 268–276. doi:https://doi.org/10.1038/35065725.

[57] A. Sanfeliu, K.-S. Fu, A distance measure between attributed relational graphs for pattern recognition, IEEE transactions on systems, man, and cybernetics (3) (1983) 353–362. doi:https://doi.org/10.1109/TSMC.1983.6313167.

[58] Z. Huang, Link prediction based on graph topology: The predictive value of generalized clustering coefficient, Available at SSRN 1634014 (2010). doi:https://dx.doi.org/10.2139/ssrn.1634014.

[59] Y. Cui, X. Wang, J. Li, Detecting overlapping communities in networks using the maximal sub-graph and the clustering coefficient, Physica A: Statistical Mechanics and its Applications 405 (2014) 85–91. doi:https://doi.org/10.1016/j.physa.2014.03.027.

[60] S. F. Nilsson, C. Reidhav, K. Lygnerud, S. Werner, Sparse district-heating in sweden, Applied Energy 85 (7) (2008) 555–564. doi:https://doi.org/10.1016/j.apenergy.2007.07.011.

[61] I. Dochev, I. Peters, H. Seller, G. K. Schuchardt, Analysing district heating potential with linear heat density. a case study from hamburg., Energy Procedia 149 (2018) 410–419. doi:https://doi.org/10.1016/j.egypro.2018.08.205.

[62] M. J. Gidden, D. Huppmann, pyam: a python package for the analysis and visualization of models of the interaction of climate, human, and environmental systems, Journal of Open Source Software 4 (33) (2019) 1095. doi:https://doi.org/10.21105/joss.01095.

[63] D. Huppmann, M. Gidden, Z. Nicholls, J. Hörsch, R. Lamboll, P. Kishimoto, T. Burandt, O. Fricko, E. Byers, J. Kikstra, et al., pyam: Analysis and visualisation of integrated assessment and macro-energy scenarios, Open Research Europe 1 (2021) e74. doi:https://doi.org/10.12688/openreseurope.13633.1.

[64] A. Hagberg, P. Swart, D. S Chult, Exploring network structure, dynamics, and function using NetworkX, retrieved on 04.09.2021, https://www.osti.gov/biblio/960616 (2008).

[65] H. Auer, P. C. del Granado, D. Huppmann, P.-Y. Oei, K. Hainsch, K. Löffler, T. Burandt, Quantitative Scenarios for Low Carbon Futures of the Pan-European Energy System, Deliverable D3.1, openENTRANCE, https://openentrance.eu/ (2020).

[66] H. Auer, P. C. del Granado, P.-Y. Oei, K. Hainsch, K. Löffler, T. Burandt, D. Huppmann, I. Grabaak, Development and modelling of different decarbonization scenarios of the European energy system until 2050 as a contribution to achieving the ambitious 1.5°C climate target–establishment

of open source/data modelling in the European H2020 project openENTRANCE, e & i Elektrotechnik und Informationstechnik (2020) 1–13. doi:https://doi.org/10.1007/s00502-020-00832-7.

[67] T. Burandt, K. Löffler, K. Hainsch, GENeSYS-MOD v2.0 - Enhancing the Global Energy System Model: Model improvements, framework changes, and European data set, Tech. rep., DIW Data Documentation (2018).

[68] D. Huppmann, E. Kriegler, V. Krey, IAMC 1.5°C Scenario Explorer and Data hosted by IIASA, retrieved on 04.09.2021, https://data.ene.iiasa.ac.at/iamc-1.5c-explorer/ (2019).

Appendix A. Data and further empirical settings

	Description	Data availability	Data source
GENeSYS-MOD v2.0	Heat generation by source	[68]	[31]
Austrian population density	in 2019	*Statistik Austria*	
Austrian population	in 2050	*Eurostat*	

Table A.1: Empirical data settings

Appendix B. Further methodology illustrations

Figure B.1 shows an illustrative example of the iterative downscaling algorithm (Algorithm 2). It shows two different conditions of a simple graph. In the first condition (i), the network topology consists of four nodes (A-D) and four lines. It is shown in the subfigure in the top left. The table below (bottom left) shows the amount of centralized and on-site heat supply as well as the indicator value for each node. Note that the numbers are only for illustration. Node A has the lowest indicator value (see marker [1] in the left table) and, therefore, its amount of centralized heat supply (marker [2]) is reallocated to the remaining nodes of the network (marker [3]). This process increases the on-site heat supply accordingly at node A as this node is not connected to the network in condition

$i + 1$ and increases the amount of centralized heat supply at nodes B-D (see the larger nodes in the top right subfigure). The heat demand of node A in condition $i + 1$ is covered only by on-site heat supply. Node A is removed from the graph and thus disconnected from the network.

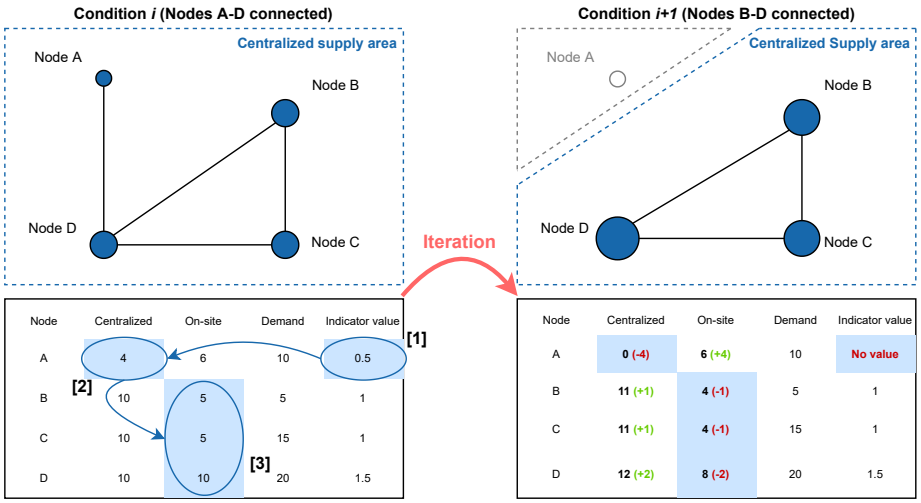

Figure B.1: Illustrative example of Algorithm 2 showing a simple graph with four nodes in two different conditions. The node with the lowest indicator value in condition i (node A) is removed from the graph (markers [1]-[3] in the table at the bottom left). The amount of centralized heat supply from node A is reallocated to the remaining nodes B-D (see table at the bottom right).